Quantum Transport Simulations of InGaAs HEMTs: Influence of mass variations on the device performance

Neophytos Neophytou, and Hans Kosina
Institute for Microelectronics, TU Wien
Gußhausstraße 27-29/E360, A-1040
Wien, Austria
e-mail: {neophytou|kosina}@iue.tuwien.ac.at

Titash Rakshit
Intel Corporation
Hillsboro, Oregon, USA

Abstract— **This paper presents a simulation work of $In_{0.7}Ga_{0.3}As$ HEMT devices for logic applications using a quantum ballistic 2D simulator based on the non-equilibrium Green's function (NEGF) approach coupled to a 2D Poisson for the electrostatics. In a previous study, we showed that $In_{0.7}Ga_{0.3}As$ short channel HEMT devices operates close to the ballistic limit and can be modeled as a ballistic channel attached to two series resistances. Since the electronic structure of the quantized channel is not known precisely, or can be altered by strain fields, in this work, we quantify our results, by investigating the variation in device performance due to variations in the effective mass values. We conclude that for these devices, variations in the electronic structure do not impact the device performance significantly. The results also provide insight into the expected effect of strain on the performance due to mass variations.**

I. INTRODUCTION

Field-effect transistors with III-V channel materials have recently received much attention because of their potential as switching devices for future low-voltage, digital technology nodes. The low effective mass and high mobility of the III-V compounds should boost the ballistic carrier velocity and improve the I_D-V_D characteristics. High-performance HEMTs based on III-V compounds with channel lengths below 90 nm have recently been demonstrated [1, 2, 3]. This work presents a continuation to our recent analysis of the HEMT devices reported by Kim et al. [1], in which we concluded that a III-V HEMT device of gate length L_G=60nm can, to first order, be seen as a ballistic channel with series resistances attached to its two ends [4]. The analysis was based on a ballistic quantum simulator based on the non-equilibrium Green's function (NEGF) technique. The electronic structure of the 15nm thick channel was described in the effective mass approximation, which was extracted from atomistic tight-binding (TB) calculations. In principle, however, the effective mass is not precisely known for ultra-thin body, ternary compound devices, and varies with the exact material composition, strain fields and distortions in the devices, which are also not known precisely. Channel thickness, and potentially, the exact placement of the atoms are unknown as well. In order to quantify the results in [4], we identify the uncertainties in the performance resulting from uncertainties in the electronic structure, described by the transport, transverse and quantization masses. We conclude that for the III-V HEMT devices, variations in the electronic structure do not affect the device performance significantly.

II. APPROACH

A. Device Geometry

The non-equilibrium Green's function approach [5] for ballistic quantum transport, utilizing a real-space Hamiltonian, is self-consistently coupled to a 2D Poisson solver for treatment of the electrostatics. For simulation purposes, the device geometry was simplified as shown in Fig. 1. The simulated HEMT consists of a 15nm $In_{0.7}Ga_{0.3}As$ layer between two $In_{0.52}Al_{0.48}As$ barrier layers as described in [1]. The gate electrode in the simulated device is placed on top of the $In_{0.52}Al_{0.48}As$ layer. A silicon δ-doped layer in the $In_{0.52}Al_{0.48}As$ barrier layer effectively dopes the source/drain regions of the device, that extend from the gate edge to the edge of the ohmic contact (denoted L_{side} in Fig. 1a, located below the n+ region), to $2.1x10^{12}/cm^2$ [6]. The δ-doped layer is located 3nm away from the channel layer.

In the experimental device [1], the source and drain ohmic contacts are located on the top of the device, and the current flow is two-dimensional through a doped heterostructure stack. Rather than attempting to simulate the contacts (and the associated metal-semiconductor contact resistance), we placed ideal contacts at the two ends of the channel as shown in Fig. 1a and added extrinsic series resistors to the source and drain. Figure 1b, shows a typical band diagram of a cross section in the middle of the channel under high gate bias conditions. An energy minimum is located in the $In_{0.52}Al_{0.48}As$ barrier layer (left) at the point of the δ-doped layer. The barrier thickness in this example is t_{ins}=7 to demonstrate the effect of the δ-doped layer on the electrostatic profile of the device. In the rest of the analysis, t_{ins}=3nm is used. It is evident here that most of the charge is localized within the channel layer, and very little penetrates into the $In_{0.52}Al_{0.48}As$ barrier layer. Figure 1c shows a typical energy resolved electron density extracted from the

978-1-4244-3927-0/09/$25.00 ©2009 IEEE

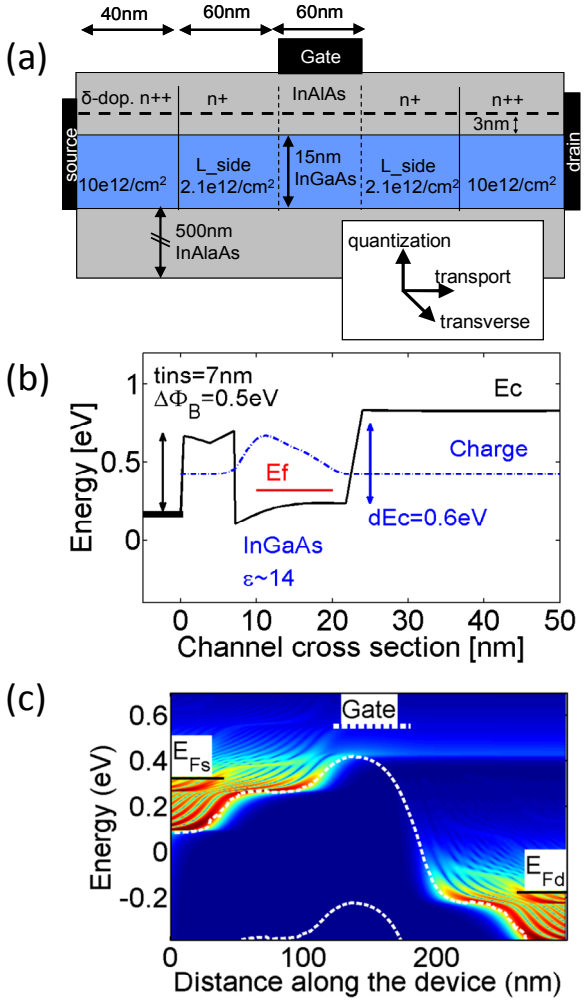

Figure 1. (a) Schematic of the HEMT device simulated with the relevant directions noted. (b) The band profile through a cross section in the center of the channel. (c) The energy resolved electron density spectrum, calculated using NEGF.

NEGF simulations. A large concentration of electrons is observed in the source/drain L_{side} regions, whereas a larger concentration is located in the far left/right regions that resemble the ohmic contacts.

B. Mass increase due to quantization

The effective mass tensor of the $In_{0.7}Ga_{0.3}As$ channel is an input to the simulation. Because of conduction band non-parabolicity, quantum confinement will increase the transport and quantization effective masses as compared to the bulk values [7]. Figure 2 demonstrates the mass variations of InAs quantum wells as a function of the well thickness. The dispersion of InAs is calculated using the $sp^3d^5s^*$ atomistic TB model. The lowest subband is then fit with a parabolic dispersion that best approximates the dispersion up to 0.2eV above the subband edge. The quantization mass is calculated from the shift of the subband edge from the bulk value as the quantum well is quantized according to 2D quantization of parabolic bands. The masses, therefore, include the effect of non-parabolicity in an approximate way. The masses in the

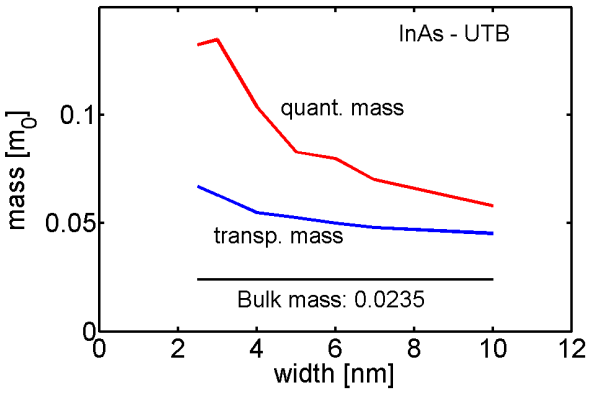

Figure 2. Transport and quantization mass variations in InAs as a function of the quantum well thickness. The transverse mass is the same as the transport mass.

InAs case increase as the well is thickness is reduced. Although the Γ valley of GaAs is more parabolic, and the mass deviation from bulk is smaller, the mass increase will appear in the In rich $In_{0.7}Ga_{0.3}As$ channel, too. Extracting the appropriate effective mass in the $In_{0.7}Ga_{0.3}As$ channels, however, is a more difficult task than in InAs channels because the masses can be a function of the exact placement of the atoms in the structure and the distortions and strain fields within the structure. In this work, we calculate the dispersion of the 15nm wide $In_{0.7}Ga_{0.3}As$ quantum well using atomistic TB calculations without assuming any lattice distortions. We extract the masses that best fit the dispersion up to 0.2eV above the conduction band edge. An effective mass of $m^* = 0.048m_0$ was calculated and used in the simulations. The mass value is higher than the weighted average of the bulk masses of InAs and GaAs in $In_{0.7}Ga_{0.3}As$ ($m^* = 0.037m_0$). That mass value is very similar to the weighted average mass value of the quantized 15nm wide InAs and GaAs quantum wells. The L valleys are very high in energy and are, therefore, ignored in our simulations.

III. RESULTS

Although we believe that the estimation of the masses is valid, by varying the masses +/- 30%, we calculate the uncertainties in the performance (ON-current) of the HEMT device due to uncertainties in the effective masses. We perform this analysis for the transport, quantization and transverse masses. Figure 3 shows the I_D-V_D characteristics extracted from the simulator (diamond-square/blue), and the experimentally measured ones (dotted/red) for the t_{ins}=3nm and L_G=60nm device presented in [1]. In the ballistic simulations we used two input parameters. The first is the value of the gate workfunction such that the comparison is performed at the same gate overdrive. The second is a series resistance that is added to the ballistic I_D-V_D to match the slope of the experimental I_D-V_D at high gate bias, since R_{SD} is an important part of HEMT devices (details in [4]). Although the ballistic I_{ON} is very close to the experimental results at lower V_G, at higher V_G the ballistic results overestimate the experimental measurements. Figures 3a, b, c show the change in the I_D-V_D as the transport, quantization and transverse masses, respectively, vary by 30%. It is evident that large

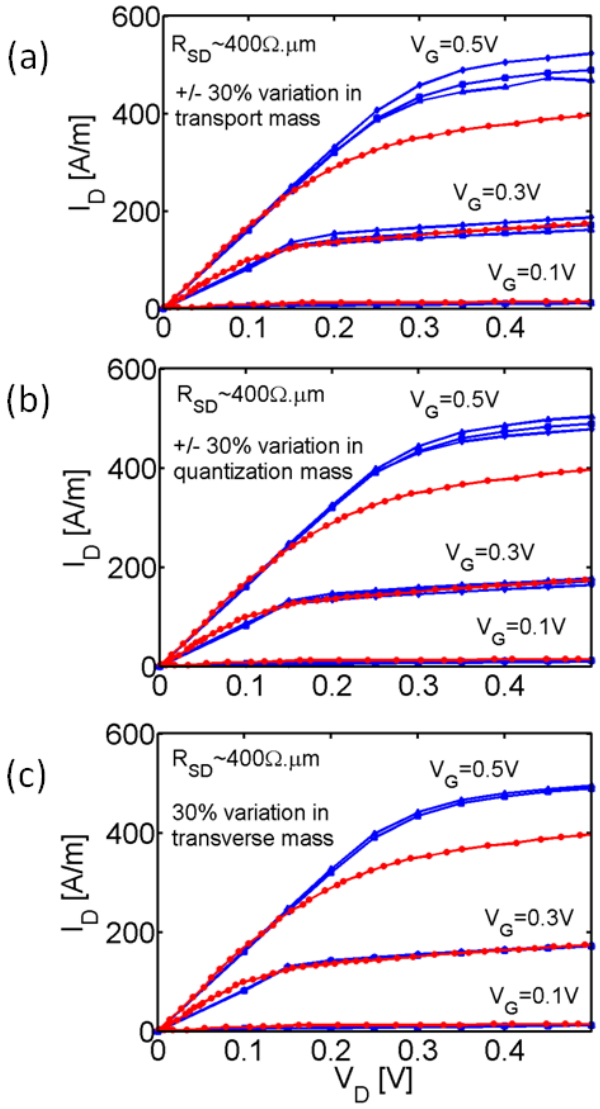

Figure 3. I_D-V_D characteristics for the experimental device (dot/red) and the simulated one (diamond-square/blue). The various simulated lines at every V_G represent results with a specific directional component of the mass tensor varying by +/-30%: Variations in the (a) transport, (b) quantization, and (c) transverse masses.

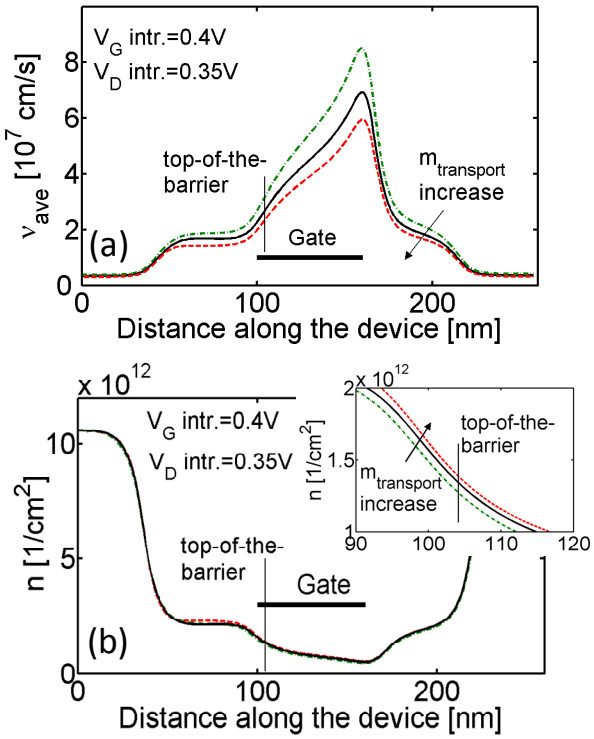

Figure 4. Internal device features at ON-state, V_G=0.4V, V_D=0.35V, corresponding to the V_G=V_D=0.5V bias of the external device. Devices are considered for which the transverse and quantization masses are kept at the reference value m*=0.048m_0, whereas the transport mass varies as m*=0.032m_0 (green/dash), 0.048m_0 (black/solid), 0.064m_0 (red/dash). The top of the barrier, and the position of the gate are indicated. (a) The carrier average velocity along the channel. (b) The charge density along the channel.

uncertainties in the mass tensor input parameters do not affect the performance significantly. Especially in the case of variations in the quantization or transverse masses (Fig. 3 b, c), that can have an impact on the capacitance of the device, very small performance variations are observed (~2% variation in ON-current with a 30% mass variation).

IV. Discussion

The largest performance variation is observed in the case of transport mass variation (+/-6%). This indicates that strain can potentially offer enhancement in the device performance, although only limited. In the ballistic limit, the current can be calculated as the product of the charge times the carrier injection velocity at the top of the energy barrier for electrons near the source region (see Fig. 1c). At this point in the channel the gate has the most effective control. Details on its exact calculation are provided in [4]. Figure 4a shows the average velocity of carriers in the channel at ON-state for the device in which the transport mass only is varied. At ON-state, the externally applied biases are V_G=V_D=0.5V. We plot the velocities at the internal to the device biases (V_G=0.4V and V_D=0.35V), thus extracting the biases that drop across the R_{SD}. The top of the barrier is indicated at 104.5nm in the channel. The velocities for the devices with m*=0.032m_0, 0.048m_0 and 0.064m_0 are v_{ave}=3.18x10^7, 2.7x10^7, and 2.36x10^7 cm/s respectively extracted from a full NEGF-Poisson. These are 18% increase and 12% decrease from the reference/middle velocity value. The charge density at the top of the barrier, on the other hand (Fig. 4b), shows much less sensitivity to variations in the effective mass values. The heavier mass channel results in a higher density of states (DOS) and a higher carrier concentration in the channel. However, the charge in the channel only partly depends on the DOS of the channel, although the device operates close to the quantum capacitance regime [4]. The barrier capacitance and the spread of the wave function in the channel (placement of charge centroid) play a large role, too [7]. Variations in the charge due to mass variations are, therefore, limited. This is similar to the minimal I_D variations observed in Fig. 3b, c in which case the mass variations only affect the devices' DOS, and little and only indirectly the carrier velocities. The charge

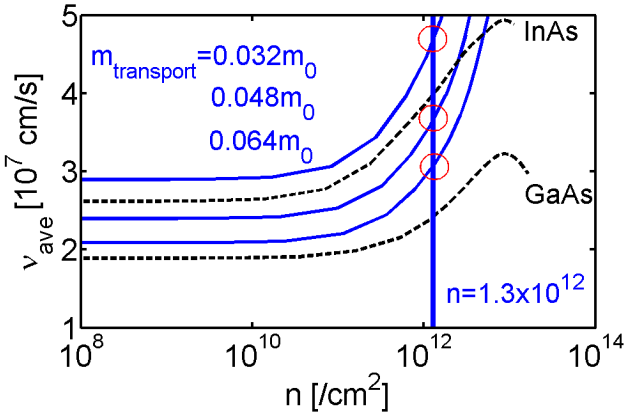

Figure 5. The bandstructure velocity vs. charge density of carriers for the devices with transverse and quantization masses kept at the reference m*=0.048m0, where the transport mass changes as m*=0.032m_0, 0.048m_0, and 0.064m_0 (blue, from top to bottom). The velocities of InAs and GaAs 15nm wide quantum wells are shown (black/dashed). Values are indicated at the n=1.3x10^{12}/cm^2.

at the top of the barrier in Fig. 4b for the devices with m*=0.032m_0, 0.048m_0 and 0.064m_0 is n=1.26x10^{12}, 1.3x10^{12}, and 1.37x10^{12} /cm^2 respectively (onset of Fig. 4b). These are 5% decrease and 3% increase from the reference/middle charge value.

The velocity variations from the middle value are expected and agree well with variations based on the non-degenerate limit velocity relation $v_{inj} = \sqrt{2k_B T / \pi m}$. The absolute value of the velocities, however, does not follow this formula, since the device operates in the degenerate limit, and is a strong function of tunneling and quantum mechanical reflections at the top of the barrier in the channel. Figure 5 shows the bandstructure velocity versus the charge density in the channel calculated using a semiclassical ballistic model. We assume that only the positive going k-states are occupied, and calculate the carrier velocities at a specific inversion carrier density. The bandstructure velocities of the devices with varying transport effective mass, while keeping the transverse and quantization masses at the reference value, are shown (blue/solid). For reference, in black/dashed we show the 15nm quantum well InAs and GaAs bandstructure velocities (the bandstructure for InAs and GaAs is calculated using TB). At n=1.3x10^{12}/cm^2, the inversion charge at ON-state in the devices described (Fig. 4b), the velocities for the devices with m*=0.032m_0, 0.048m_0 and 0.064m_0 are v_{ave}=4.7x10^7, 3.6x10^7, and 3.08x10^{7}cm/s respectively. These values are all higher than the velocity values calculated in the full quantum mechanical simulation. In NEGF, quantum mechanical reflections result in occupation of negative going k-states that reduces the average velocity. Tunneling is another factor that reduces the velocities in the full simulations.

The bandstructure velocities for the heavier mass channels (m*=0.048m_0, 0.064m_0) are within the InAs and GaAs 15nm quantum well velocities. The light mass channel (m*=0.032m_0) has a velocity greater than the InAs channel. Although it is more reasonable that the mass in the $In_{0.7}Ga_{0.3}As$ channel will be less than the InAs mass, lighter masses can be achieved with strained materials, and pure InAs channels. The expected velocity, and I_{ON} enhancement will be moderate, however, since quantum mechanical effects tend to decrease the carrier velocity.

V. Conclusion

A simulation approach for a III-V HEMT device, using the NEGF approach, coupled to a 2D Poisson solver is described. The simulation results are calibrated to the experimental data described in Ref. [1]. Other than the complicated ohmic contacts, the rest of the device is described in the simulations as close as possible to the experimental one. The gate workfunction and series resistances were used as fitting parameters to match the V_T and the total resistance in the simulated and experimental data. The effective mass tensor used in the simulations to describe the electronic structure of the device is extracted from atomistic TB calculations. The masses are heavier than the bulk masses because of non-parabolicity. Due to the complexity of the $In_{0.7}Ga_{0.3}As$ channel, which includes distortions, strain fields and quantization in the channel, its electronic structure is not precisely known. This uncertainty in the electronic structure, however, does not affect the device performance significantly. Variations in the quantization and transverse masses (+/- 30%) have insignificant effect on the ON-current compared. Only the transport mass variations have some effect on the ON-current. These results indicate that performance improvement will be only moderate if the effective mass of III-V HEMTs is reduced due to strain or the use of pure InAs channels with lighter mass.

Acknowledgment

This work has been partially supported by funds from the Austrian Science Fund, FWF, contract I79-N16. Resources of the Network for Computational Nanotechnology (NCN, nanoHUB.org) were used for this work. N. Neophytou would like to thank Prof. Mark Lundstrom of Purdue University for elaborated discussions.

References

[1] D.-H. Kim and J. del Alamo, "Scaling behavior of $In_{0.7}Ga_{0.3}As$ HEMTs for logic," 2006 International Electron Devices Meeting, p. 837, 2006.

[2] D.-H. Kim and J. del Alamo, "Logic performance of 40nm InAs HEMTs," 2007 International Electron Devices Meeting, p. 629, 2007.

[3] R. Chau, S. Datta, M. Doczy, B. Doyle, B. Jin, J. Kavalieros, A. Majumdar, M. Metz, M. Radosavljevic, "Benchmarking nanotechnology for high performance and low-power logic transistor applications," IEEE Trans. Nanotechnol., vol. 4, no. 2, pp. 153-158, March 2005.

[4] N. Neophytou, T. Rakshit, and M. S. Lundstrom, "Performance Analysis of 60nm gate length III-V InGaAs HEMTs: Simulations vs. Experiments" to appear in TED, 2009, also in arXiv: 0810.1540 (Oct. 2008).

[5] S. Datta, Electronic Transport in Mesoscopic Systems. Cambridge MA: Cambridge Univ. Press, 1997.

[6] Personal communication with Dr. Dae-Hyun Kim and Prof. Jesus del Alamo.

[7] N. Neophytou, A. Paul, M. Lundstrom, and G. Klimeck, "Bandstructure effects in silicon nanowire electron transport," IEEE Trans. Elect. Dev., vol. 55, no. 6, pp. 1286-1297, 2008.